PAPER • **OPEN ACCESS**

A model for computing thermally-driven shallow flows

To cite this article: Isabel Echeverribar *et al* 2023 *IOP Conf. Ser.: Earth Environ. Sci.* **1136** 012037

A model for computing thermally-driven shallow flows

Isabel Echeverribar[1,2], Sergio Martínez-Aranda[1], Javier Fernández-Pato[1,2], Reinaldo García[2], Pilar Brufau[1] and Pilar García-Navarro[1]

[1] Fluid Mechanics, I3A-Universidad de Zaragoza, Zaragoza, 50018, Spain
[2] Hydronia Europe, Madrid, 28046, Spain

echeverribar@unizar.es

Abstract. In many natural disasters such as overland oil spills or lava flows, physical fluid properties as density change when considering non-homogeneous spatial and time variable distributions of the temperature. This effect is even more remarkable when these flows show a non-Newtonian behaviour due to the sensitivity of their rheological properties as viscosity or yield stress to temperature. In these cases, temperature becomes a significant variable that drives the fluid behaviour, which must be solved using an energy equation coupled with the free surface flow system. Special attention is devoted to thermal source terms which must include all the heat fluid exchanges, and their modelling sometimes can govern the complete flow behaviour. Fluid density, viscosity and yield stress, also affected by temperature, must be recomputed every time step. Summarizing, this work presents a 2D free surface flow model considering density and temperature variations, which could even modify viscosity and yield stress, with heat transfer mechanisms. The model is applied to oil spill overland simulations and heating/cooling test cases are carried out to ensure the system energy balance. As conclusions, it can be said that the numerical results demonstrate the importance of the heat exchange effects and those of the density, viscosity and yield stress variations.

1. Introduction

When dealing with surface geophysical flows, such as oil spills, landslides, muddy slurries, lava flows, etc, the choice of the system of equations to solve depends on the type of phenomena to be reproduced. Generally, these kind of free surface non-Newtonian viscoplastic flows are widely addressed with the depth-averaged shallow-type models. Traditionally, these models assume a hydrostatic pressure distribution in the flow column and incompressible flow, dismissing density variations that might affect the flow dynamics. However, when the flow is governed by a non-uniform distribution of a driven property, such as temperature, the bulk properties of the flow column vary in time and space, and hence the incompressible flow assumption is no longer valid.

In these kinds of phenomena, the flow density, which depends on temperature, turns into an important variable which must be coupled with the rest of variables within the system of equations. On one hand, compressible shallow-flow models have been recently developed for mud/debris flows [1-4], and solid-laden currents [5,6], where the bulk density of the flow column is mainly controlled by the volumetric concentration of solid particles. As important differences were found between the results provided by incompressible and compressible models [4] when density is governed by particle concentration, temperature might have the same effects on fluids at high temperatures, such the oil of an oil spill. On the other hand, the temperature is often considered as a passively transported scalar with no influence

on the fluid dynamics [7,8] or, when special attention is paid into the temperature, the system dynamics are coarsely modelled or estimated [9,10].

This work presents a model for incompressible flows developed for fluids with a high particle concentration but using temperature as the variable on which the density depends. The mathematical approach has unconditional hyperbolic character, which allows solving it as in [11]. This represents a decisive advantage in order to develop efficient numerical models able to deal with realistic large-scale long-term geophysical events.

2. Simulation model: equations and numerical scheme

2.1. System of equations

The mathematical model that describes the behaviour of the oil flow is compound by a mass conservation equation, two momentum equations in *x* and *y* directions and a final temperature transport equation that derives from energy conservation equation:

$$\begin{gathered}\frac{\partial(\rho h)}{\partial t}+\frac{\partial(\rho hu)}{\partial x}+\frac{\partial(\rho hv)}{\partial y}=0\\ \frac{\partial(\rho hu)}{\partial t}+\frac{\partial}{\partial x}\left(\rho hu^2+\frac{1}{2}\rho gh^2\right)+\frac{\partial}{\partial y}(\rho huv)=-g\rho h\frac{\partial z_b}{\partial x}-\tau_{bx}\\ \frac{\partial(\rho hv)}{\partial t}+\frac{\partial}{\partial x}(\rho huv)+\frac{\partial}{\partial y}\left(\rho hv^2+\frac{1}{2}\rho gh^2\right)=-g\rho h\frac{\partial z_b}{\partial y}-\tau_{by}\\ \frac{\partial(hT)}{\partial t}+\frac{\partial(huT)}{\partial x}+\frac{\partial(hvT)}{\partial y}=\boldsymbol{S}_T\end{gathered} \tag{1}$$

where ρ stands for the density, h represents water depth and u and v are the velocities in x and y directions, and T stands for fluid temperature. The temperature source term, S_T, considers the heat transfer with the environment as in Echeverribar et al. 2022. The closure equation relates density and temperature, and updates also viscosity and yield stress as

$$\begin{gathered}\rho(T)=\rho_0+K\,(T-T_0)\\ YS(T)=10^{(Ays\,T^2+Bys\,T+Cys)}\\ \mu(T)=A_\mu+\frac{B_\mu}{T}\end{gathered} \tag{2}$$

where parameters of the expressions come from experimental works to characterize oils. Finally, it is important to note that both, viscosity and yield stress, affect directly to friction stresses in momentum equations following a particular formulation. To compute stresses in equation (1) as a function of yield stress and viscosity of equation (2) a Simplified Bingham Model has been chosen in this case.

The source term is divided into two components as

$$S_T=\frac{\dot{Q}}{\rho hC_p}=\frac{\dot{Q}_{rad}+\dot{Q}_{conv}}{\rho hC_p} \tag{3}$$

where Q_{rad} stands for the solar radiation that falls upon the flow and Q_{conv} represents the convection heat losses, that are modelled as:

$$\dot{Q}_{conv}=h_c(T-T_{air}) \tag{4}$$

where h_c the convection coefficient in $Wm^{-2}K$ and Tair the air temperature, in K. The emitted solar radiation is neglected in this oil spill application, although it can be important when simulating other fluid such as lava.

2.2. Numerical scheme

To solve the system, the final model is written in terms of a normalized density, r, and a normalized temperature, T^{∇}, as:

$$\begin{gathered}\frac{\partial(rh)}{\partial t}+\frac{\partial(rhu)}{\partial x}+\frac{\partial(rhv)}{\partial y}=0\\ \frac{\partial(rhu)}{\partial t}+\frac{\partial}{\partial x}\left(rhu^2+\frac{1}{2}rgh^2\right)+\frac{\partial}{\partial y}(rhuv)=-grh\frac{\partial z_b}{\partial x}-\frac{\tau_{bx}}{\rho_0}\\ \frac{\partial(rhv)}{\partial t}+\frac{\partial}{\partial x}(rhuv)+\frac{\partial}{\partial y}\left(\rho hv^2+\frac{1}{2}rgh^2\right)=-grh\frac{\partial z_b}{\partial y}-\frac{\tau_{by}}{\rho_0}\\ \frac{\partial(hT^{\nabla})}{\partial t}+\frac{\partial(huT^{\nabla})}{\partial x}+\frac{\partial(hvT^{\nabla})}{\partial y}=0\end{gathered} \tag{5}$$

while the final temperature is updated decoupled with the source term with:

$$\frac{\partial T}{\partial t}=\frac{\dot{Q}}{\rho hC_p}=\boldsymbol{S}_T \tag{6}$$

Therefore, the updating scheme for the conserved variables follows:

$$U_i^{n+1}=U_i^n-\frac{\Delta t}{A_i}\sum_{k=1}^{NE}\mathbf{R}_k^{-1}\boldsymbol{\mathcal{F}}_k^{\downarrow-}l_k \tag{7}$$

where $\boldsymbol{\mathcal{F}}_k^{\downarrow-}$ is a defined augmented flux vector through the kth wall, which includes the convective fluxes and the momentum source term contributions as:

$$\boldsymbol{\mathcal{F}}_k^{\downarrow-}=\mathbf{F}\left(\hat{\mathbf{U}}_i^n\right)+\sum_{m-}\left[\left(\tilde{\lambda}_m\tilde{\alpha}_m-\tilde{\beta}_m-\tilde{\sigma}_m\right)\tilde{\mathbf{e}}_m\right]_k^n \tag{8}$$

where $\left(\tilde{\lambda}_m\right)_k^n$ are the eigenvalues of the Jacobian matrix of the local Riemann problem, which stand for the wave celerities of the system; $(\tilde{\mathbf{e}}_m)_k^n$ are the eigen vectors associated to that values; $(\tilde{\alpha}_m)_k^n$ are the wave strengths; and $\left(\tilde{\beta}_m\right)_k^n$ and $(\tilde{\sigma}_m)_k^n$ denote the source strengths including bed slope and basal resistance, respectively. Since an explicit numerical scheme is being used, the time step size is restricted by the Courant-Friedrichs-Levy (CFL) number, which lead to a stability condition as

$$\Delta t=\mathrm{CFL}\min_k\left(\frac{\mathrm{MIN}\left(A_i,A_j\right)}{l_k\max_m\left(\left|\tilde{\lambda}_m\right|\right)_k^n}\right) \tag{9}$$

This CFL number must be bounded between 0 and 1 for 2D triangular meshes.

3. Circular dam-break test case

3.1. Test case description

A 2D circular dam break is simulated on a 10 km square flat domain. The initial cylindrical fluid column has a diameter of 1000 m and a height of 52 m. The properties relating temperature and density following equation (2) are a reference temperature of 20ºC (T_0), a density at that temperature of 860 kg/m^3 (ρ_0), and a proportionality constant, *K*, of -1. Two different initial temperatures are considered to stablish two different cases: 35 and 50 ºC. The relationship between viscosity and yield stress with temperature is modelled by pairs of values on a table instead of using expression (2). The values can be found in Table 1.

The case is simulated on an unstructured triangular mesh of 105182 elements. The simulation runs for 360 s with a CFL of 0.95. No thermal source terms have been considered in this case.

Table 1. Variations of yield stress and viscosity with temperature.

Temperature [ºC]	Yield stress [Pa]	Temperature [ºC]	Viscosity [Pa s]
35	2000	35	0.362
40	200	55	0.138
45	20	60	0.110
50	0.02	65	0.086

3.2. Numerical results

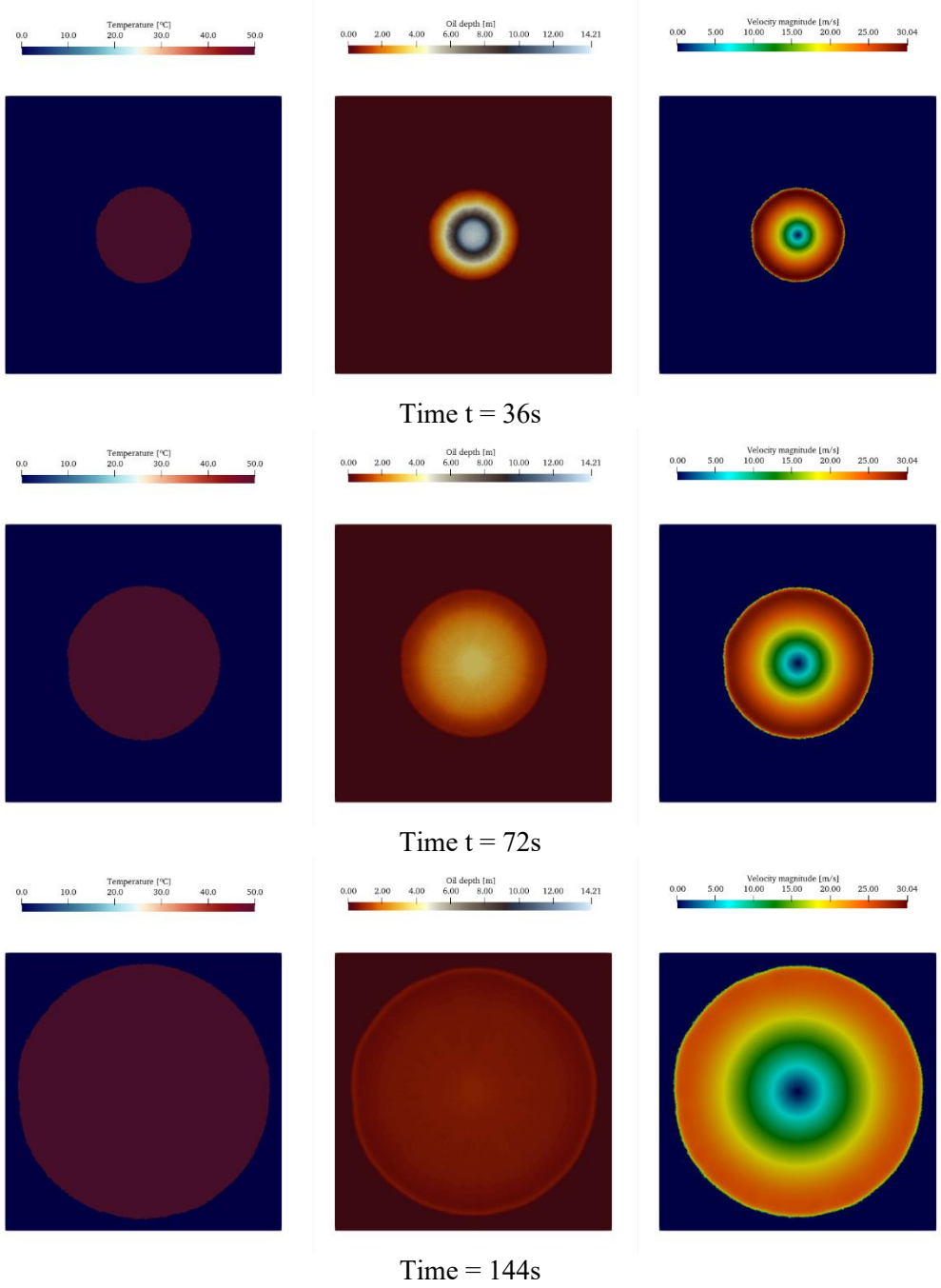

Figure 1: Spatial distribution of temperature (left), oil depth (centre) and velocity magnitude (right) for an oil at 50ºC.

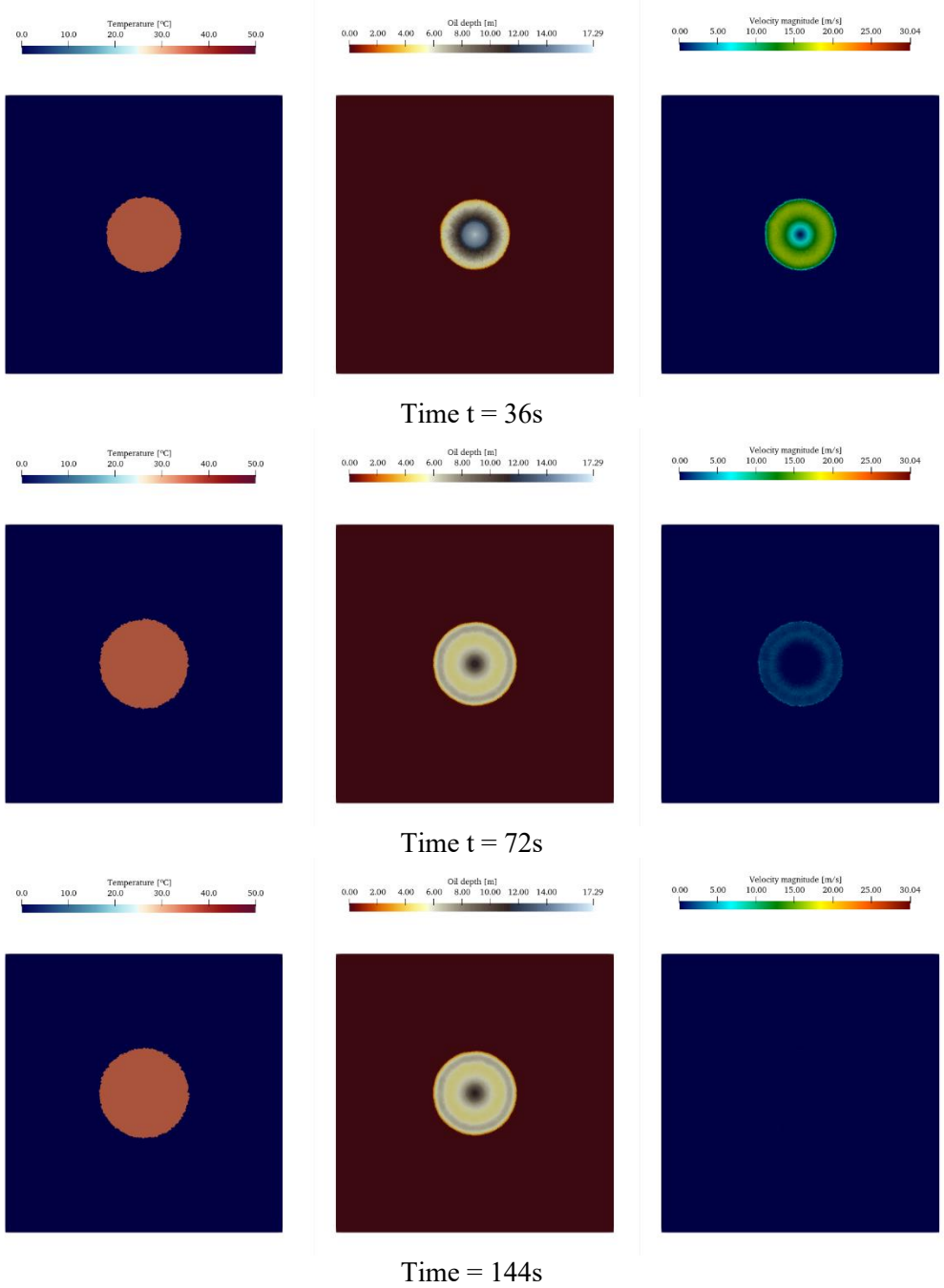

Figure 2: Spatial distribution of temperature (left), oil depth (centre) and velocity magnitude (right) for an oil at 35ºC.

The initial condition is the same in both cases except for the temperature, which causes variations in the rheological properties of the fluid and its density. Figure 1 shows the results of dam break for an initial temperature of 50 ºC at different times. The left column of pictures shows the fluid temperature, constant at 50ºC due to the absence of heat source terms. In the centre is represented the fluid depth, which remains thicker in the centre while in the periphery begins to reduce. The right column shows the magnitude of the velocity, which is lower in the centre and increases radially, decreasing just at the periphery due to the advance of the dry front. It is observed that at 72 and 144 s the stain advances maintaining a radial symmetry and the same behaviour. At 144 s, in the fluid depth, an over-elevation

of the surface begins to be observed in the periphery together with a decrease in the velocity caused by the yield stress.

Figure 2 shows the same type of results as in Figure 1 for an initial temperature of 35 ºC. Being lower than in the previous case, yield stress, density and viscosity are much higher, following equation (2) and Table 1. Thus, it is observed that the velocities are much lower and the expansion of the oil slick is much smaller. A comparison between cases in terms of fluid depth can be seen on Figure 3, where the longitudinal profile of oil depth is represented for both cases at different time levels. In both figures, it is seen how for an initial temperature of 35ºC the yield stress reaches such high values that the fluid is completely stopped at 144 s without a large expansion.

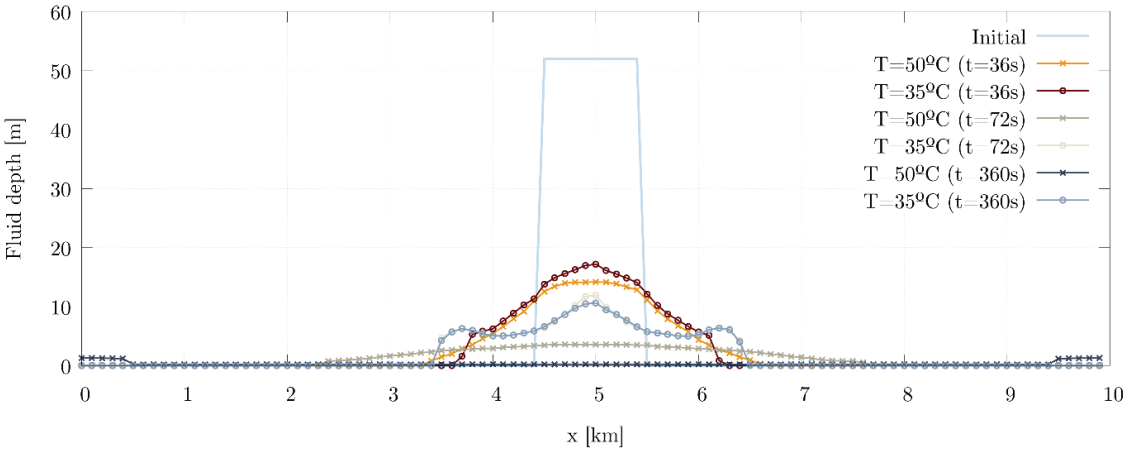

Figure 3: Longitudinal profile of oil depth in the circular dam-break for different times and different temperatures: 35ºC (-o-) and 50ºC (-×-).

4. Algeciras overland oil spill test case

4.1. Test case description

A digital terrain model of the Algeciras port, where exist an oil station, has been used to simulate an eventual overland oil spill. The model has been prepared to deal with wet/dry fronts to simulate overland oil spills. The necessity of considering the spatial distribution of temperature, density and heat transfer is clearly demonstrated on the results. Two different cases are simulated: environment A, with no wind (low convection coefficient), normal air temperature and solar radiation; and environment B, with high wind speed, low air temperature and no solar radiation.

Table 2. Environmental characteristics of the simulation cases.

	Environment A	**Environment B**
Initial temperature	85ºC	85ºC
Air temperature	40ºC	10ºC
Radiation	1000 W/m^2	0 W/m^2

4.2. Numerical results

The spill is simulated for 20 h and the flooding slick is analysed then as well as its temperature distribution. The triangular mesh contains 35581 elements and the simulations are carried out with a CFL of 0.9.

Figure 4 shows the different temperature distribution provoked by two oil sources at the same temperature spilled on two different environments. In this case, the differences on the flooded area are provoked by differences on yield stress and viscosity –both influenced by temperature, which changes

depending on the environment-. Colder environments provoking important heat transferences lead to high yield stress, cold oil and reduced flooded areas.

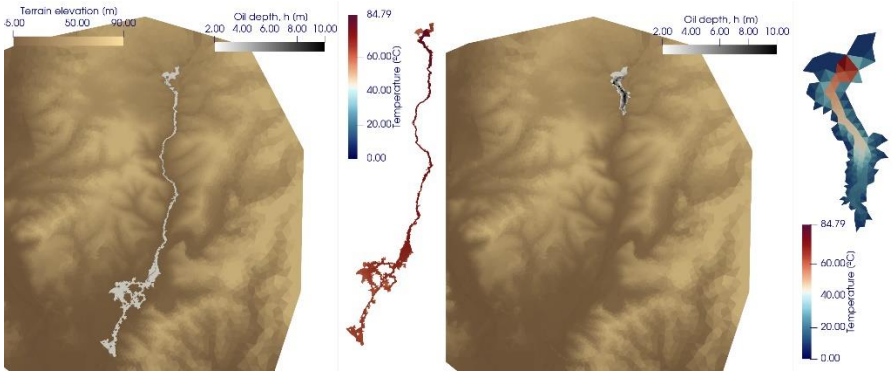

Figure 4: Flooded area and temperature at t = 20 h of an overland oil spill for the same oil into environment A (left) and B (right).

5. Conclusions

When dealing with high temperature non-Newtonian flows, the treatment of density and temperature variation considerations entails a difference on the results. A model of temperature-dependent flows has been developed and applied to oil spill simulations. It has been proved how a combination of both heat transfer and density/temperature changes affect the rheological properties of the flow, which affect the friction law when using models such as the Bingham model. The model has been applied first to a theoretical dam break to show a different evolution depending on the fluid temperature, although remaining constant. Additionally, a real test case of an oil spill has been simulated in different surrounding conditions to test the influence of heat transfer. It has been shown that initial inertial forces provoke a fast movement that later slows down due to a shear stress that depends on temperature, which varies depending on the heat transfer. The necessity of these models to simulate thermally-driven flows has been proved.

The sensitivity to temperature of the model allows to simulate different rheological flows such as crude oil or lava flows. However, further research must be done to develop more sophisticated heat transfer models or take evaporation into account.

Acknowledgments

Authors wish to acknowledge Hydronia Europe for the collaboration. This work was partially funded by the Spanish Ministry of Science and Innovation under the research project PGC2018-094341-B-I00. This work has also been partially funded by Gobierno de Aragón through Fondo Social Europeo (T32-20R, Feder 2014–2020 “Construyendo Europa desde Aragón”).

References

[1] Kowalski J and McElwaine 2013 Shallow two-component gravity-driven flows with vertical variation *Journal of Fluid Mechanics*, **714** pp 434-462 https://doi.org/10.1017/jfm.2012.489

[2] Xia C, Li J, Cao Z, Liu Q and Hu K 2018 A quasi single-phase model for debris flows and its comparison with a two-phase model *Journal of Mountain Science*, **15**(5) pp 1071-1089 https://doi.org/10.1007/s11629-018-4886-5

[3] Martínez-Aranda S, Murillo J and García-Navarro P 2020 A robust two-dimensional model for highly sediment-laden unsteady flows of variable density over movable beds *Journal of Hydroinformatics* **22**(5) pp 1138-1160 https://doi.org/10.1016/j.enggeo.2021.106462

[4] Martínez-Aranda S, Murillo J and García-Navarro P 2021 A GPU-accelerated Efficient Simulation Tool (EST) for 2D variable-density mud/debris flows over non-uniform erodible beds *Engineering Geology* **296** pp 106462 https://doi.org/10.1016/j.enggeo.2021.106462

[5] Murillo J, Latorre B and García-Navarro P 2012 A Riemann solver for unsteady computation of 2D shallow flows with variable density *Journal of Computational Physics* **231** pp 4775-4807 https://doi.org/10.1016/j.jcp.2012.03.016
[6] Cao Z, Xia C, Pender G and Liu Q 2017 Shallow water hydrosediment-morphodynamic equations for fluvial processes *Jounral of Hydraulic Engineering* **143**(5) pp 02517001 https://doi.org/10.1061/(ASCE)HY.1943-7900.0001281
[7] Kim K S and Chapra S C 1997 Temperature model for highly transient shallow streams *Journal of Hydraulic Engineering* **123**(1) pp 30-40
[8] Cea L, Bermúdez M, Puertas J, Bladé E, Corestein G, Escolano E, Conde A, Bockelmann-Evans B and Ahmadian R 2016 IberWQ: new simulation tool for 2D water quality modelling in rivers and shallow estuaries *Journal of Hydroinformatics* **18**(5) pp 816-830 https://doi.org/10.2166/hydro.2016.235
[9] Ramírez-Camacho J G, Carbone F, Pastor E, Bubbico R and Casal J 2017 Assesing the consequences of pipeline accidents to support land-use planning *Safety Scince* **97** pp 34-42 https://doi.org/10.1016/j.ssci.2016.01.021
[10] Chen C, Li C, Reniers G and Yang F 2021 Safety and security of oil and gas pipeline transportation: A systematic analysis of research trends ans future needs using wos *Journal of Cleaner Production* **279** pp 123583 https://doi.org/10.1016/j.jclepro.2020.123583
[11] Echeverribar I, Morales-Hernández M, Brufau P and García-Navarro P 2019 2D numerical simulation of unsteady flows for large scale floods prediction in real time *Advances in water resources* **134** p 103444 https://doi.org/10.1016/j.advwatres.2019.103444